Available online at www.sciencedirect.com
ScienceDirect
International Journal of Thermal Sciences 46 (2007) 1056–1063
International Journal of Thermal Sciences
www.elsevier.com/locate/ijts

Experimental study of the dynamic behaviour of a porous medium submitted to a wall heat flux in view of thermal energy storage by sensible heat

B. Dhifaoui [a], S. Ben Jabrallah [a,b], A. Belghith [a], J.P. Corriou [c,*]

[a] *Faculté des Sciences de Tunis, Laboratoire des Transferts de Chaleur et de Masse, Campus Universitaire, 1060 Tunis, Tunisia*
[b] *Faculté des Sciences de Bizerte, 7021 Bizerte, Tunisia*
[c] *Laboratoire des Sciences de Génie Chimique, CNRS-ENSIC-INPL, 1, rue Grandville, BP 20451, 54001 Nancy cedex, France*

Received 29 September 2006; received in revised form 16 November 2006; accepted 17 November 2006

Available online 26 March 2007

Abstract

This study concerns the storage of thermal energy in a porous bed mainly formed by a vertical channel, filled with glass beads, heated on one of the vertical walls by a constant heat flux. The use of glass beads is motivated by the possible use of such a system for storage of solar energy by sensitive heat and its optimization. The medium is characterized by a large thermal inertia which favors a slow return of the heat stored during the heating phase. After model reduction, the system can be dynamically modeled as a simple first order which allows us to evaluate the heat transfer coefficient and to predict its response to real values of the solar flux. The system efficiency defined as the ratio of the stored energy to the energy provided increases with the storage volume and decreases with the return time for fixed width and storage time.

Keywords: Energy storage; Sensitive heat; Solar energy; Porous medium; Natural convection; Dynamics

1. Introduction

The irregular character of solar energy induces serious limitations in many potential applications. As a solution to remedy to these limitations, the storage of thermal energy will find an increasing number of uses as the energetic level of the storage processes is improved as well as the capacity of their reservoirs which depends on the thermal characteristics of the concerned material such as its fusion enthalpy and its heat capacity, on the storage volumes and the insulation of the storage tank. Thermal energy can be stored as latent heat of sensitive heat or both together [8].

Several types of energy accumulators based on latent heat have been designed [1,6,10,11], however they present some drawbacks like the necessity of reaching the operating point of the system, i.e. its fusion temperature, the complexity of the phenomena of change of phase, the non-homogeneity of the fusion medium and the degradation of material with time due to numerous fusion–solidification cycles. Thus the energy storage under sensitive heat form, in spite of the voluminous aspect and the necessity of working at high temperatures, remains nowadays the most used type. The choice of the storage medium is generally related to the system, in general water when the heat conducting fluid (the coolant) is liquid and stone beds when the coolant is hot air. Porous media have been the subject of numerous studies which can be fundamental, numerical and experimental. Many books have also been published among which [7,9,13,16].

Bechki et al. [2] studied the behaviour of a vertical gravel bed, cooled or heated by air, with respect to both heating and cooling. The transfer coefficients measured at different bed heights were correlated with respect to the air flow rate by relation: $h = cG^{0.77}$ where parameter c is 25.7 in heating case and 27.2 in cooling case. Forestier et al. [5] have shown by means of numerical modeling performed in natural convection that the results obtained by a pure conductive model or a model taking into account convection are very close.

* Corresponding author.
E-mail address: corriou@ensic.inpl-nancy.fr (J.P. Corriou).

1290-0729/$ – see front matter
doi:10.1016/j.ijthermalsci.2006.11.014

Nomenclature

A	geometric form factor $= H/L$	
C_p	heat capacity at constant pressure	$\mathrm{J\,kg^{-1}\,K^{-1}}$
d_B	diameter of the beads	m
H	height of the channel	m
h	heat transfer coefficient	$\mathrm{W\,m^{-2}\,K^{-1}}$
K	permeability	$\mathrm{m^{-2}}$
l	depth of the channel	m
L	width of the channel	m
Nu	Nusselt number	
P	power	W
$\dot{Q}_f$	flux density given to the system	$\mathrm{W\,m^{-2}}$
Ra	Rayleigh number	
S	surface area of the heated plate	$\mathrm{m^2}$
T	temperature	K or °C
T_y	mean temperature at height y	K or °C
t	time	s
(x, y)	Cartesian coordinates	m

Greek symbols

β	heat expansion coefficient	$\mathrm{K^{-1}}$
λ	thermal conductivity	$\mathrm{W\,m^{-1}\,K^{-1}}$
μ	dynamic viscosity	Pa s
ν	kinematic viscosity	$\mathrm{m^2\,s^{-1}}$
ρ	density	$\mathrm{kg\,m^{-3}}$

Subscripts

ad	relative to the quasi-adiabatic wall
am	ambient
c	relative to the heated wall
ch	charge
disch	discharge
e	inlet
eff	effective
F	fluid (air)
fi	final state
i	initial state
m	porous medium
p	plate
S	solid (beads)
s	outlet
sat	saturation
st	storage

Benmansour and Hamdan [3] defined in a numerical study the efficiency η of a porous bed as the ratio

$$\eta = \frac{T_m - T_a}{T_e - T_a}$$

where T_m, T_a and T_e are respectively the temperatures of medium, ambient and entering fluid, crossed by a previously heated fluid. They showed that η increases with the storage volume and that the duration necessary for the bed to reach thermal saturation decreases with the Reynolds number.

Works in natural convection have been performed in confined media [1,6,8,10] while those in forced convection have been performed in open media [2,3,5]. The case of an open system is rarely studied in natural convection. Bennasrallah et al. [4]; Slimi and Bennasrallah [14] have studied numerically unsteady natural convection in a cylinder filled with particles, open at its extremities and with its wall heated by a constant heat flux. In both works, the heat exchange coefficient, concerning the exchanges between the porous medium and environment has been imposed by the choice of a Biot number $Bio = Hh/\lambda_{\mathrm{eff}}$ defined as the ratio of the product of the transfer coefficient by the medium height over the effective conductivity of the porous medium.

The objective of the present study is to optimize the storage of energy by sensitive heat in a fixed porous bed. Such a system of heat energy storage could be implemented in housing (heating floors) or in the absorbers of plane sensors. The advantage of this system is its heat capacity larger than $10^6\ \mathrm{J\,K^{-1}\,kg^{-1}}$, which results in a relatively high return time for stored energy and its robustness with respect to a periodic operation.

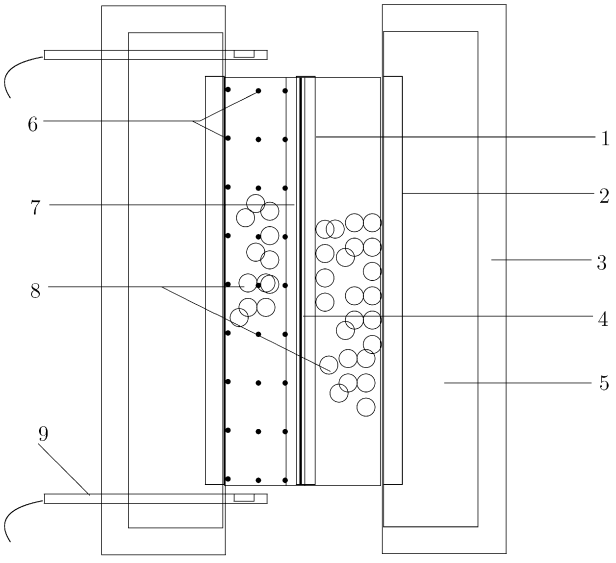

Fig. 1. Scheme of the porous channel. 1: heated plate, 2: quasi-adiabatic plate, 3: wooden frame, 4: resistance made of carbon sheets, 5: thermal insulator (cork), 6: type K thermocouples, 7: Samicanite plates (electrical insulator), 8: glass beads, 9: probes (hot wire anemometer).

2. Experimental setup

The experimental setup mainly comprises a vertical parallelepiped channel of form factor $A = H/L$ that will be varied during this study, while the height is maintained constant. One of the vertical walls of this channel having dimensions 40 cm $\times$ 20 cm is heated by a constant flux while the parallel wall is considered adiabatic (Fig. 1). The channel thus formed is filled by an heterogeneous packing of glass beads to consti-

tute the porous medium which is the object of the study. The temperatures of the active plates forming the channel as well as the temperature inside the medium are measured by type K thermocouples of low diameter. The simultaneous distribution of the velocity and of the temperature of the heating fluid (air) crossing the solid matrix is measured by means of probes (hot wire anemometer). The measurements are automatically recorded and treated by adequate calculation codes. The charge corresponds to the phase of application of a constant heat flux while the discharge is the phase following the charge when no heat flux is applied and the porous medium releases its heat contents to the environment. The modes of charge and discharge of the system are controlled by following the evolution of the temperature of the different sensors with a given sampling period. Before usage, the thermocouples connected to a centralized system with resolution $\pm 0.1\,^{\circ}\mathrm{C}$ are calibrated by means of a thermostated bath.

3. Characteristics of the porous medium

- *Porosity*. The porosity of the medium is defined as the ratio of the volume of fluid over the total volume of the channel. It is given [17] as

$$\varepsilon = \varepsilon_{\infty}\left(1 + \frac{0.568 d_b}{L(1 - \exp(\frac{-3L}{d_b}))}\right) \tag{1}$$

where ε_{∞} is the porosity far from the walls of the channel of width L and d_b is the diameter of the beads forming the solid matrix of the medium.

- *Heat capacity*. The heat capacity of the porous medium is an arithmetic mean of the capacities of the solid and of the fluid

$$(\rho C_p)_m = (1-\varepsilon)(\rho C_p)_S + \varepsilon(\rho C_p)_F \tag{2}$$

- *Thermal conductivity*. The effective heat conductivity of the medium is given by the relation of [18]

$$\frac{\lambda_{\text{eff}}}{\lambda_F} = \left[1 - \sqrt{1-\varepsilon} + 2\frac{\sqrt{1-\varepsilon}}{1-\lambda C}\left(\frac{(1-\lambda)C}{(1-\lambda C)^2}\log\left(\frac{1}{\lambda C}\right) - \frac{C+1}{2} - \frac{C-1}{1-\lambda C}\right)\right] \tag{3}$$

with

$$\lambda = \frac{\lambda_{\text{eff}}}{\lambda_F}; \qquad C = 1.25\left(\frac{1-\varepsilon}{\varepsilon}\right)^{10/9} \tag{4}$$

λ_F and λ_S represent respectively the heat conductivities of the fluid and of the solid matrix.

- *Thermal parameters*. The values of the densities and of the heat capacities of air and of the solid as glass beads are given by literature. For the air density, a mean value with respect to temperature is chosen. The density and the heat of the solids depend little on temperature (Table 1).

4. Energy balance of the storage system

The different terms of power (simply designed below as heat) intervening in the energy balance of the storage element (Fig. 2) are respectively

Table 1
Physical properties of various materials

	Air 40 °C	Glass 20 °C	Stainless steel 20 °C
λ [W m^{-1} K^{-1}]	0.0272	0.78	16.3
ρ [kg m^{-3}]	1.127	2700	7816
C_p [J kg^{-1} K^{-1}]	1007	840	460
ν [m^2 s^{-1}]	2.4×10^{-5}	–	–

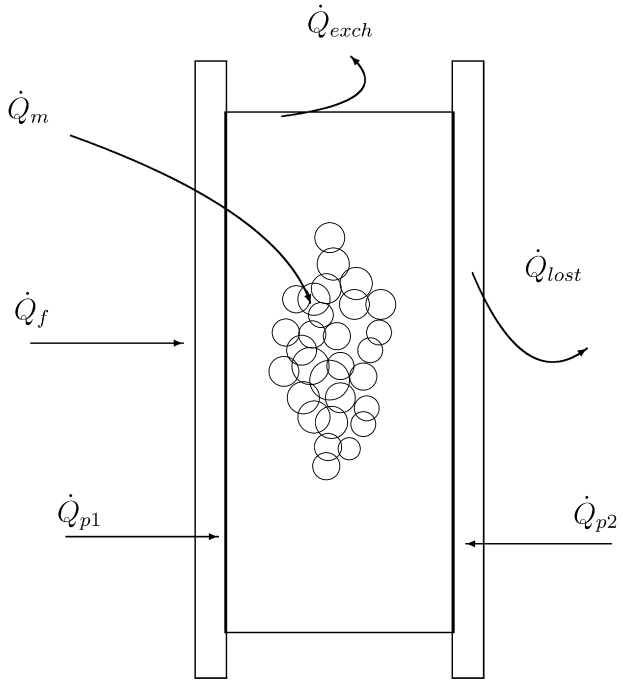

Fig. 2. Energy balance. $\dot{Q}_f$: heat given to the system, $\dot{Q}_{\text{lost}}$: heat lost through the insulators, $\dot{Q}_{\text{exch}}$: heat exchanged between the medium and the outside, $\dot{Q}_m$: heat accumulated in the porous medium, $\dot{Q}_{p1}$: heat accumulated in the heated plate, $\dot{Q}_{p2}$: heat accumulated in the quasi-adiabatic plate.

- the heat given to the system per unit of heating surface area

$$\dot{Q}_f = \frac{P}{S} \tag{5}$$

where P is the given power and S the surface area of the heated plate;

- the sensitive heat accumulated in the plates forming the active faces of the channel

$$\dot{Q}_p = \frac{V_p(\rho C_p)_p}{S}\left(\frac{d\overline{T}_{p1}}{dt} + \frac{d\overline{T}_{p2}}{dt}\right) \tag{6}$$

where V_p, ρ, C_p, $\overline{T}_{p1}$ and $\overline{T}_{p2}$ are respectively the volume, density, heat capacity, and mean temperatures of the heated and adiabatic plates;

- the sensitive heat accumulated in the porous medium

$$\dot{Q}_m = \frac{V_m(\rho C_p)_m}{S}\frac{d\overline{T}_m}{dt} \tag{7}$$

- the heat exchanged with the environment through the upper face of the medium

$$\dot{Q}_{\text{exch}} = h(\overline{T}_s - T_a) \tag{8}$$

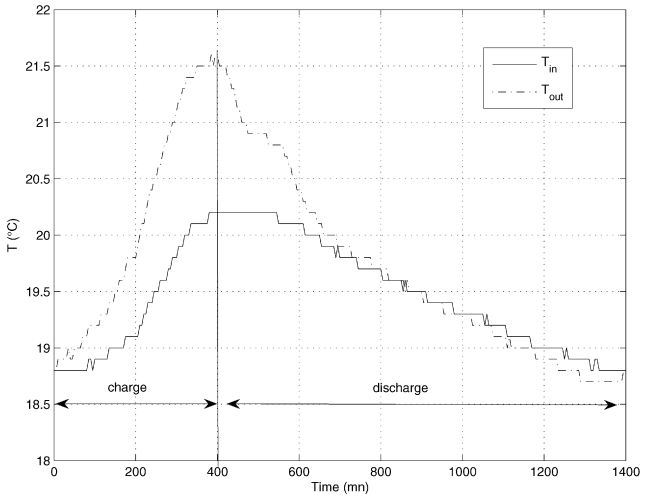

Fig. 3. Evolution of the fluid temperature at the inlet and at the outlet of the porous medium during a process of charge, then discharge ($\dot{Q}_f = 250\ \mathrm{W\,m^{-2}}$, $d_B = 10$ mm and $L = 7$ cm).

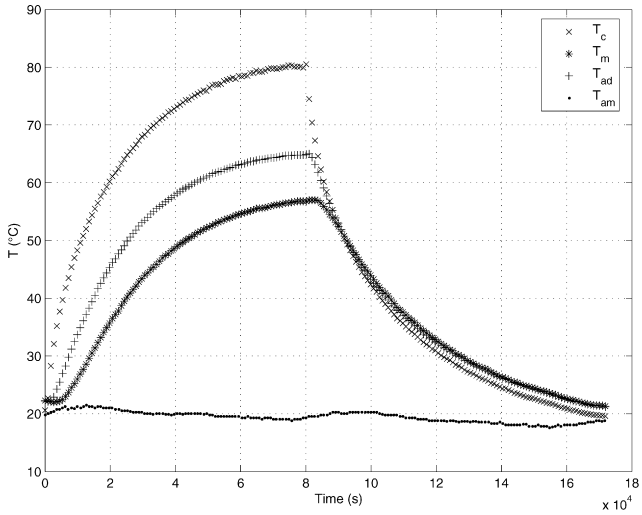

Fig. 4. Evolution of the temperatures of the medium, of both plates and of ambient air during a cycle: a charge followed by a discharge ($\dot{Q}_f = 250\ \mathrm{W\,m^{-2}}$, $d_B = 10$ mm and $L = 7$ cm).

where T_s and T_a are respectively the temperatures of the upper face of the medium and ambient;

- the heat lost by the system through the thermal insulator

$$\dot{Q}_{\text{lost}} = \frac{1}{R}(\overline{T}_{p2} - T_a) \tag{9}$$

R is the thermal resistance of the insulator.

Taking into account Eqs. (5)–(9), the energy balance of the storage element is

$$\dot{Q}_f = \frac{V_p(\rho C_p)_p}{S}\left(\frac{d\overline{T}_{p1}}{dt} + \frac{d\overline{T}_{p2}}{dt}\right) + \frac{1}{R}(\overline{T}_{p_2} - T_a) + h(\overline{T}_s - T_a) + \frac{V_m(\rho C_p)_m}{S}\frac{d\overline{T}_m}{dt} \tag{10}$$

5. Experimental results and dynamic modeling

Several experiments have been performed to verify the two-dimensional character of the studied problem. In most cases, the deviation between the values recorded by three thermocouples located at mid-height of the heated wall does not overcome 2%, which allows us to consider the flow as two-dimensional.

5.1. Thermal behaviour of the system and modeling as first order

Fig. 4 represents respectively the evolutions of the temperatures of the heated wall, of the adiabatic wall and of the medium during a cycle constituted by charging followed by discharging for a fixed width ($L = 7$ cm). The system requires more than 20 hours to reach the steady state (full charge) and thus shows the high thermal inertia of the system. To come back to its initial state (full discharge in open air), it needs more than 25 hours.

To improve the characterization of the evolution of the system, the temperatures at the inlet and at the outlet of the porous medium have been recorded during charge and discharge (Fig. 3). These temperatures have been recorded by fast

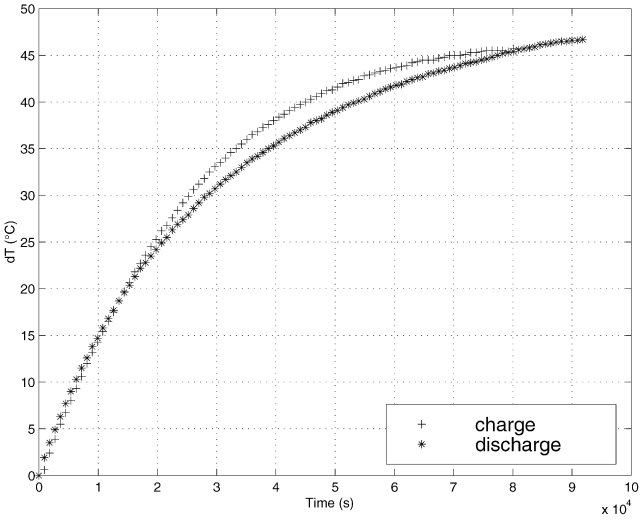

Fig. 5. Comparison of the absolute deviation temperature of the system during both processes of charge and discharge ($\dot{Q}_f = 250\ \mathrm{W\,m^{-2}}$, $d_B = 10$ mm and $L = 7$ cm).

sensors placed for the inlet at 2 cm from the grid supporting the solid matrix, for the outlet at 5 cm over the upper surface of the porous medium. However, the variation of these temperatures does not exceed 3 °C for a heat flux density equal to $250\ \mathrm{W\,m^{-2}}$, despite the large increase of temperature inside the medium. The system behaves as a reservoir of energy.

The allure of the lines of Fig. 4 let think that the system is likely to behave dynamically as a first order. To check that hypothesis, first the absolute value of the deviation $dT = T(t) - T(t_0)$, where t_0 is the initial time either for charge or discharge, is represented for a given heat flux density (Fig. 5) during both operations of charge and discharge. If the behaviour of the system were totally symmetrical for charge and discharge, both lines would superimpose. It is clear that there exists a small deviation between the charge and discharge behaviour, however

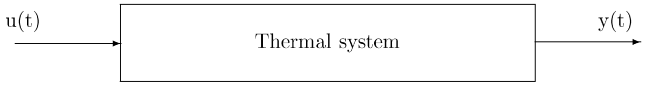

Fig. 6. First order model.

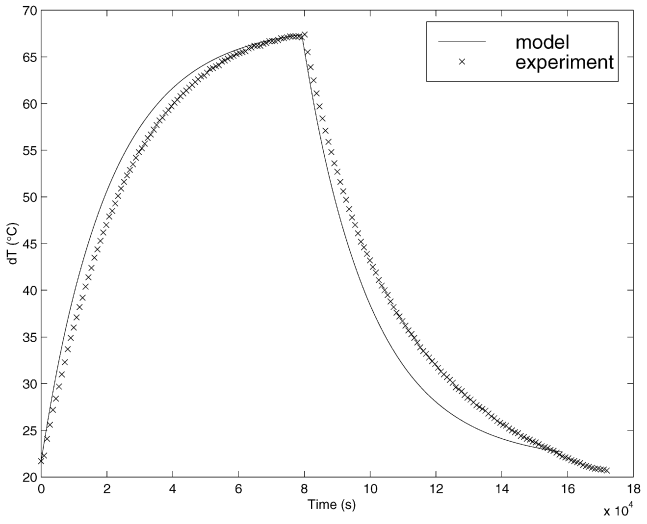

Fig. 7. Comparison model-experiment during a cycle ($\dot{Q}_f = 300$ W m^{-2}, $d_B = 10$ mm and $L = 4$ cm).

they are relatively similar. This dissymetry is characteristic of the nonlinear behaviour of the process.

Noting $u(t)$ the input function of the system (flux density) and $y(t)$ the response of the system (temperature), the dynamic behaviour of the system (Fig. 6) can be approximately represented by a first-order differential equation

$$\tau y'(t) + dy(t) = G\,du(t) \tag{11}$$

with τ the time constant and G the steady state gain (K m^{-2} W^{-1}) of the system. du and dy are deviation variables. It is supposed that at $t = 0$, the system is in steady state. Assuming that during the charge, the heat flux is applied at $t = 0$ and lasts a given time t_{ch}, the response to a step input of the heat flux density $\dot{Q}_f$ results

$$y(t) = y(0) + G\dot{Q}_f\left[1 - \exp\left(-\frac{t}{\tau_{\text{ch}}}\right)\right] \tag{12}$$

for charge with time constant τ_{ch}. If discharge follows immediately the charge, the equation for discharge is

$$y(t) = y(0) + \left[y(t_{\text{ch}}) - y(0)\right]\exp\left(-\frac{t - t_{\text{ch}}}{\tau_{\text{disch}}}\right) \tag{13}$$

with time constant τ_{disch} for discharge.

In order to verify if the hypothesis that the model is a first-order dynamic system, experiments are performed and the responses of the thermocouples implemented in the storage element are compared to those of the model resulting from Eq. (16) for a similar excitation. This comparison has been performed for different heat flux densities, various form factors and bead diameters of the porous bed. On Fig. 7 where the same gain and time constant are used for charge and discharge, a comparison of the evolution of the mean temperature of the system $\overline{T}_{\text{sys}}$ between the model and experiments is shown during a cycle, i.e. a charge followed by a discharge. A satisfactory agreement is found during the charge process, however some deviation which does not exceed 6% appears during the discharge. The system thus behaves approximately as a first-order linear process, however the time constant for charge is slightly smaller than the one for discharge.

To determine the expressions of the time constant and of the steady state gain with respect to the thermal parameters of the system, mean temperatures are considered for the various elements of the prototype. Furthermore the temperatures T_{p1}, T_{p2} of the plates, T_m of the porous medium and T_s of the upper face of the medium are assumed to be identical. Let $\overline{T}_{\text{sys}}$ be the mean global temperature of the storage element. Using this hypothesis, the energy balance of the element previously given by equation (10) becomes

$$\dot{Q}_f = \left(\frac{2V_p(\rho C_p)_p}{S} + \frac{V_m(\rho C_p)_m}{S}\right)\frac{d\overline{T}_{\text{sys}}}{dt} + \left(\frac{1}{R} + h\right)(\overline{T}_{\text{sys}} - T_a) \tag{14}$$

Set

$$u(t) = \dot{Q}_f; \qquad y(t) = \overline{T}_{\text{sys}}; \qquad y(0) = T_a$$
$$dy(t) = y(t) - y(0)$$
$$a = \frac{2V_p(\rho C_p)_p}{S} + \frac{V_m(\rho C_p)_m}{S}; \qquad b = \frac{1}{R} + h \tag{15}$$

so that Eq. (14) can be written as

$$\frac{a}{b}y'(t) + dy(t) = \frac{1}{b}du(t) \tag{16}$$

From Eqs. (11) and (16), the expressions of time constant τ and gain G with respect to the physical parameters of the system result

$$\tau = \frac{a}{b} = \frac{\frac{2V_p(\rho C_p)_p}{A} + \frac{V_m(\rho C_p)_m}{S}}{\frac{1}{R} + h}, \qquad G = \frac{1}{b} = \frac{1}{\frac{1}{R} + h} \tag{17}$$

yielding the heat transfer coefficient h

$$h = \frac{1}{G} - \frac{1}{R} \tag{18}$$

The identified parameters were $G = 0.186$ K m^2 W^{-1} and $\tau = 5.74$ h for a heat flux density equal to 250 W m^{-2}.

Thus the value of the heat transfer coefficient h is obtained from experiments by knowing the steady state gain and the thermal resistance of the concerned insulator (cork layer of thickness 16 cm and of thermal conductivity 0.04 W m^{-1} K^{-1}). The calculated heat transfer coefficient is around: $h = 5$ W m^{-2} K^{-1}. This value is neatly lower to the value used by [4,14]. The Biot number $Bio = hH/\lambda_{\text{eff}}$ relative to the thermal exchange between the upper surface of the medium and ambient air is 2000. For the present case of a medium of height 40 cm and thermal conductivity around 0.2 W m^{-1} K^{-1}, the resulting heat transfer coefficient would be 1000 W m^{-2} K^{-1}, far above the observed one. On the opposite, the observed value of the heat transfer coefficient is close to the value deduced, for low velocities, of the correlation in [12]

$$h = 5.7 + 3.8V_\infty \tag{19}$$

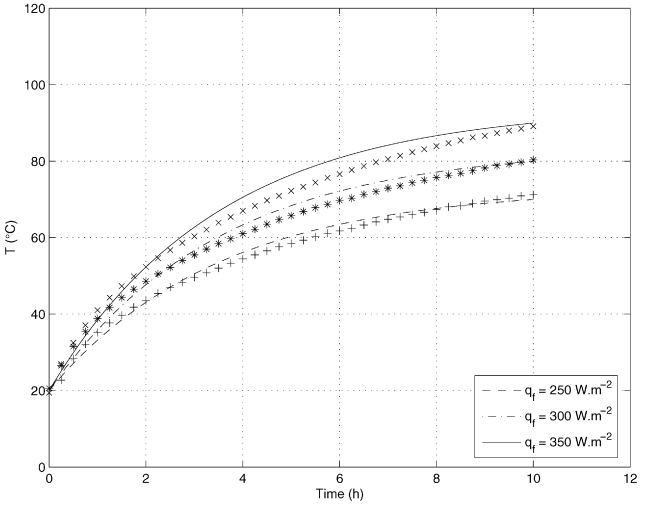

Fig. 8. Variation of the temperature of the heated wall for different values of the heat flux density ($d_B = 4$ mm and $L = 4$ cm). Continuous for model and dotted for experiments.

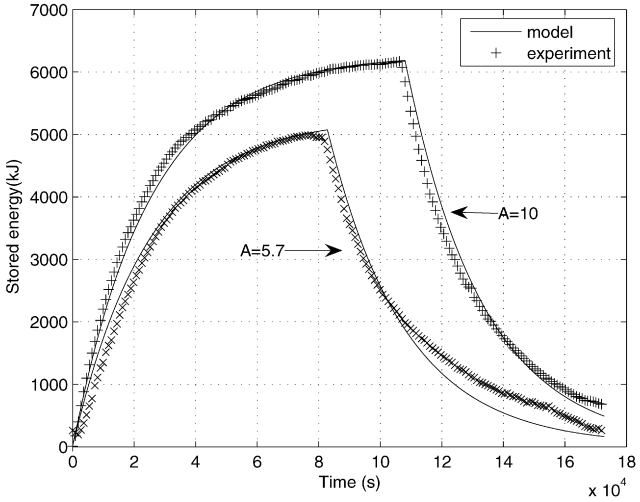

Fig. 9. Evolution of the energy stored by the system for two different form factors $A = 5.7$ and $A = 10$ ($\dot{Q}_f = 300$ W m^{-2}, $d_B = 10$ mm, $L = 4$ and $L = 7$ cm). Model: continuous lines, experiments: symbols.

where h is the heat transfer coefficient between the ground surface and air and V_∞ is the wind velocity (expressed in m s^{-1}).

Using either the full model or the approximation of the first order process, the behaviour of such a storage system can be easily simulated. The influence of the operating parameters such as the heat flux density can also be understood.

5.2. Influence of the heat flux

The evolution of the mean temperature of the heated wall has been studied for three values of the heat flux density $\dot{Q}_f$ applied to the system (Fig. 8). The allure of the lines is similar to that of the storage medium shown in Fig. 5. Again, this dynamic behaviour can be considered as a first order system. The same time constant equal to 3.5 h is considered for the three cases, a lower value than the time constant of the storage medium equal to 5.7 h. Only the steady state gain differs, depending linearly but slightly on the heat flux density as

$$G = -7 \times 10^{-5} \dot{Q}_f + 0.234 \tag{20}$$

The agreement between the three models and the corresponding experiments is satisfying, however the deviation increases slightly with the heat flux density (4.4% for 250 W m^{-2}, 5.5% for 300 W m^{-2} and 6.3% for 350 W m^{-2}). When a higher heat flux is applied, the difference between the temperatures of the various components of the system (plates, porous medium) becomes larger and the approximation of a mean temperature for the system becomes less valid.

5.3. Influence of the form factor

In Fig. 9, the lines display the evolution of the energy stored per width unit during both processes of charge and discharge for two different form factors, for a given bed height. Similar lines were obtained by [15] for a porous bed formed with steel beads. When the form factor increases, the porous medium needs more time to reach the steady state determined when the temperature fluctuation is lower than 0.2 °C. When the form factor is large and the width between the plates small, the influence of the walls becomes important and strongly reduces the ascending movement of interstitial air in the porous medium [4].

The system stores more energy per width unit for a form factor equal to 10 than for a form factor equal to 5.7 (6×10^3 kJ with respect to 5×10^3 kJ at steady state).

Indeed the energy provided to the system can be decomposed as

$$E_f = E_m + E_p + E_{\text{lost}} + E_{\text{exch}} \tag{21}$$

hence

$$E_m = E_f - (E_p + E_{\text{lost}} + E_{\text{exch}}) \tag{22}$$

with $E_{\text{exch}} = hS'(T_s - T_a)t = hLl(T_s - T_a)t$ being the energy exchanged with the ambient medium where the heat transfer coefficient h depends very little on the heat flux, the channel width L and depth l.

If it is considered that the energy stored in the walls and that lost through the insulating parts remain invariant when the form factor is varied, the energy stored in the medium decreases when the heat exchanged through the upper surface increases. However an increase of the form factor induces a decrease of the exchange surface ($S' = Ll = lH/A$) and thus induces an increase of the energy stored in the medium.

As a reference, it must be noted that the heating through its floor of a standard house of 100 m^2 of useful surface needs a heat flux density of 100 W m^{-2} [1]. This is equivalent to two elements per m^2 having a form factor equal to 5.7 or three elements having a form factor equal to 10.

5.4. Storage capacity and efficiency of the system

The efficiency of the system in the studied case is defined as the ratio of the energy E_{st} stored per width unit over the energy

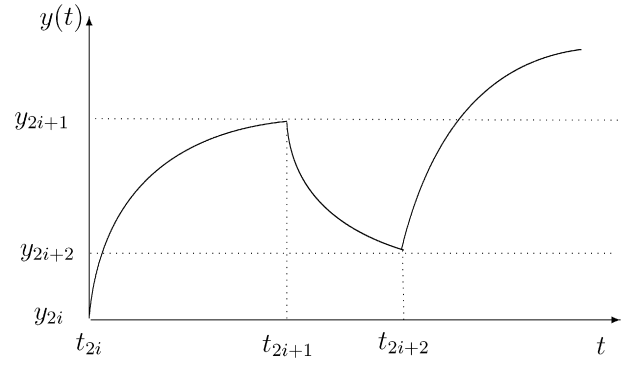

Fig. 10. Response of the system during processes of charge and discharge.

E provided to the system during a charge time t_{ch}, necessary for the system to reach asymptotically a given temperature [8]

$$\eta = \frac{E_{st}}{E} \tag{23}$$

with

$$E = \frac{P t_{ch}}{L} \quad \text{and} \quad E_{st} = S(\rho C_p)_m (T_{fi} - T_i) \tag{24}$$

For a given volume, the efficiency is all the higher as the stored heat quantity is larger and the outlet temperature of the medium remains low.

For a charge time t_{ch} equal to 22 hours corresponding to the steady state, the efficiency of the system increases from 25 to 30% when the form factor varies from 5.7 to 10 (Fig. 9).

5.5. Partial charges and discharges

Consider a sequence constituted by charges of same heat flux density $\dot{Q}_f$ followed by discharges after each charge. The initial time of charge is t_{2i} with $i \geqslant 0$, while the initial time of discharge is t_{2i+1}. During processes of partial charge and discharge (Fig. 10), the equations ruling the system result from Eqs. (12) and (13) as

Charge:

$$y_{2i}(t) = y_{2i-1}(t_{2i}) + \left[G_{2i}\dot{Q}_f - \left(y_{2i-1}(t_{2i}) - y(0)\right)\right] \times \left[1 - \exp\left(\frac{-(t - t_{2i})}{\tau_{ch}}\right)\right]$$

for $t \in [t_{2i}, t_{2i+1}]$ $(i \geqslant 0)$

Discharge:

$$y_{2i+1}(t) = y(0) + \left[y_{2i}(t_{2i+1}) - y(0)\right] \exp\left(\frac{-(t - t_{2i+1})}{\tau_{disch}}\right)$$

for $t \in [t_{2i+1}, t_{2i+2}]$ (25)

If $i = 0$, $y_{2i-1}(t_{2i})$ is $y(0)$.

Several experiments have been performed with uncomplete cycles by varying the heat power and the durations of storage and unstorage. Figs. 11 and 12 show the evolution of the temperature of the system during two sequences of partial charges and discharges which have the same charge duration equal to 2 h and two different discharge durations 2 h and 4 h. After a certain number of cycles, the temperature tends towards a limit cycle, it evolves periodically; the system loses by discharge what it receives periodically during the previous charge period. This figure also shows that the increase of the discharge duration induces a decrease of the temperature of the medium and consequently a decrease of the efficiency of the system.

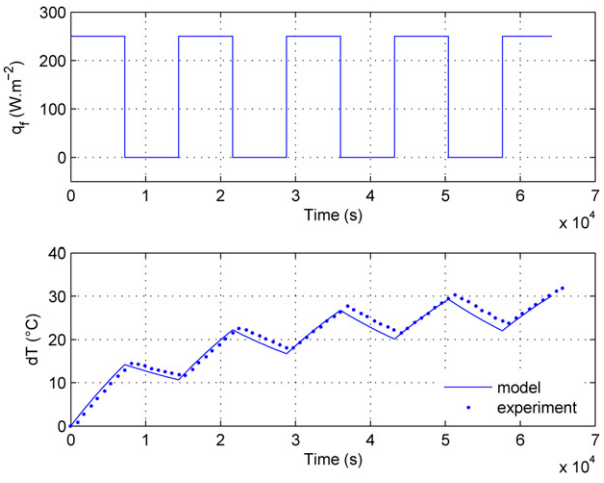

Fig. 11. Comparison model-experiments during processes of partial charges and discharges. Heat flux density (top) and variation of temperature (bottom) ($\dot{Q}_f = 250$ W m^{-2}, $d_B = 4$ mm, $L = 4$ cm, $t_{ch} = 2$ h and $t_{disch} = 2$ h).

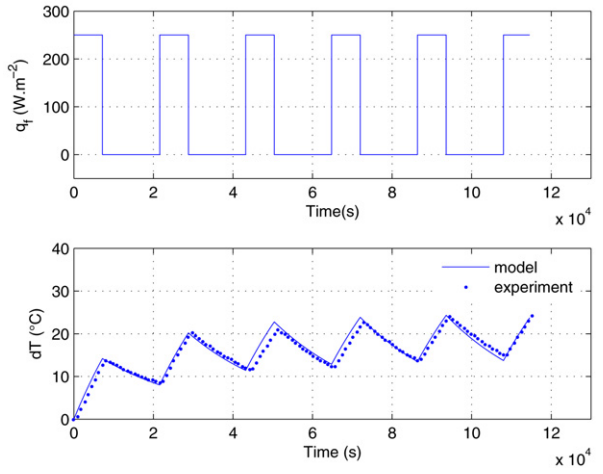

Fig. 12. Comparison model-experiments during processes of partial charges and discharges. Heat flux density (top) and variation of temperature (bottom) ($\dot{Q}_f = 250$ W m^{-2}, $d_B = 4$ mm, $L = 4$ cm, $t_{ch} = 2$ h and $t_{disch} = 4$ h).

6. Response of the system for real data of a solar flux

An interesting aspect of the prototype system lies in its potential application to the storage of solar energy as sensitive heat. Thus, real data of a solar flux have been imposed as the input of the system. The data have been taken in the region around Tunis (Tunisia) and the months of January and July have been considered in particular for their extreme characteristics. The response of the system is given on Figs. 13 and 14. They represent the variation of the mean temperature of the system with respect to the solar hour for each month. The maximum temperature is reached with some delay with respect to the maximum of the heat flux density provided to the system, it is around

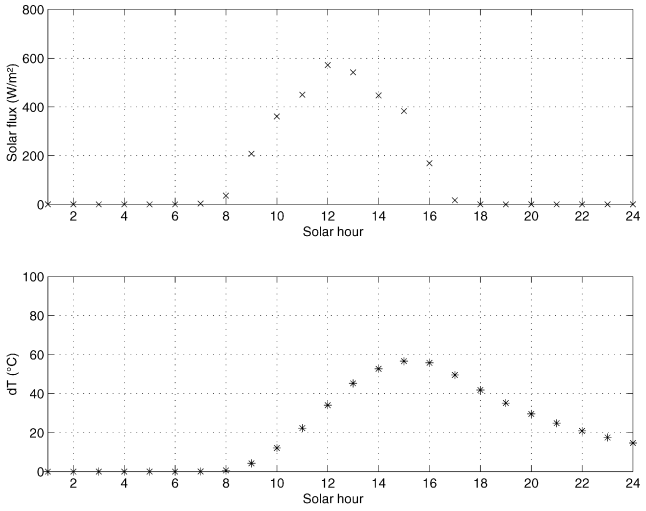

Fig. 13. Solar flux during one day of January 2004 and response of the system.

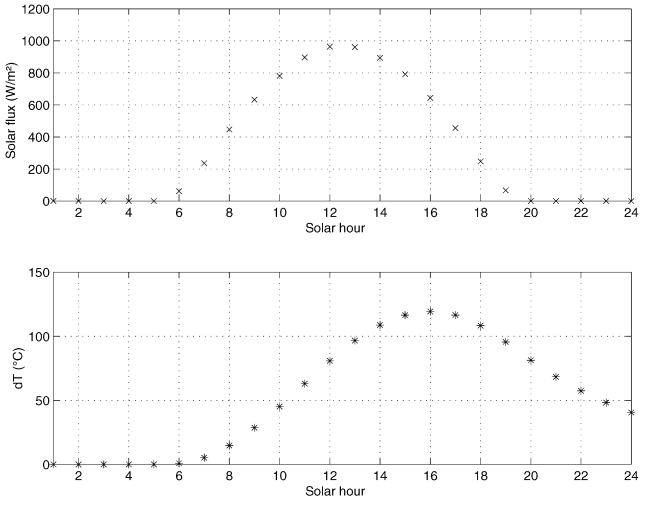

Fig. 14. Solar flux during one day of June 2004 and response of the system.

120 °C in July and 60 °C in January. The delay afore mentioned is due to the thermal inertia of the system, it is lower in January than in July (3 hours compared to 4 hours), but this is also related to the twice larger gain in July.

7. Conclusion

An experimental study of the thermal behaviour of a vertical channel filled by a porous medium constituted of glass beads and air in view of storing heat under its sensitive form is performed. A large thermal inertia of the system corresponding to the duration of its discharge is shown. The system efficiency defined as the ratio of the stored energy over the energy given to the system increases with the volume of storage and decreases with the discharge time for a fixed channel width and a fixed charge duration. This permeability of the medium induces a confinement of the fluid which has a low temperature at the outlet and increases the efficiency of the system.

The dynamic modeling of the system as a first order by comparison with the experiments allows us to evaluate the thermal heat exchange coefficient and to predict the response of the system to a heat flux corresponding to real solar data in order to reach the main objective which is the optimization of the system behaviour under a solar flux.

References

[1] M. Amir, M. Lacroix, N. Galanis, Comportement thermique de dalles chauffantes électriques pour le stockage quotidien, Int. J. Thermal Sci. 38 (1999) 121–131.

[2] D. Bechki, H. Bouguettaia, M.T. Meftah, Propriétés thermiques d'un lit fixe, La Marsa, Tunis, Tunisie, 2001.

[3] A. Benmansour, M.A. Hamdan, Simulation du stockage de l'énergie thermique dans un lit fixe de sphères contenant un matériau à changement de phase, Revue d'Energie Renouvelable 4 (2001) 125–134.

[4] S. Bennasrallah, T. Amara, M.A. Du Peuty, Convection naturelle instationnaire dans un cylindre rempli de grains ouvert à ses extrémités et dont la paroi est chauffée par un flux de chaleur constant: validité de l'hypothèse de l'équilibre thermique local, Int. J. Heat Mass Transfer 40 (1996) 1155–1168.

[5] A. Forestier, P. Forges, M. Amouroux, Simulation et optimisation des transferts thermochimiques dans un réacteur solide gaz, J. Physique III 7 (1997) 1593–1614.

[6] Z. Ait Hammou, M. Lacroix, A new PCM storage system for managing simultaneously solar and electric energy, Energy Buildings 38 (2006) 258–265.

[7] D.B. Ingham, I. Pop (Eds.), Transport Phenomena in Porous Media, vol. I, Pergamon, Oxford, 1998;
D.B. Ingham, I. Pop (Eds.), Transport Phenomena in Porous Media, vol. II, Pergamon, Oxford, 2002;
D.B. Ingham, I. Pop (Eds.), Transport Phenomena in Porous Media, vol. III, Pergamon, Oxford, 2005.

[8] M. Jocelyn, Conception, instrumentation, modélisation et analyse d'un élément de stockage d'énergie par chaleur latente, PhD thesis, Université de Sherbrooke, Sherbrooke, Canada, 1999.

[9] M. Kaviany, Principles of Heat Transfer in Porous Media, second ed., Mechanical Engineering Series, Springer, New York, 1999.

[10] A. Louadi, Transfert de chaleur dans un matériau à changement de phase: application au stockage cyclique d'énergie électrique, PhD thesis, Sherbrooke, Canada, Université de Sherbrooke, 1996.

[11] A. Louadi, M. Lacroix, Thermal performance of a latent heat energy storage ventilated panel for electric load management, Int. J. Heat Mass Transfer 42 (1999) 275–286.

[12] Y. Nassar, A. ElNoaman, A. Abutaima, S. Yousif, A. Salem, Evaluation of underground soil thermal storage properties in Libya, Renewable Energy 31 (2006) 593–598.

[13] D.A. Nield, A. Bejan, Convection in Porous Media, third ed., Springer, New York, 2006.

[14] K. Slimi, S. Bennasrallah, Transient natural convection in a vertical cylinder opened at the extremities and filled with a fluid saturated porous medium: validity of Darcy flow model and boundary layer approximations, Int. J. Heat Mass Transfer 41 (1997) 1113–1125.

[15] M. Sozen, K. Vafai, L.A. Kennedy, Thermal charging and discharging of sensible and latent heat storage packed beds, J. Thermophys. 5 (1990) 623–625.

[16] K. Vafai, H.A. Hadim (Eds.), Handbook of Porous Media, Marcel Dekker, New York, 2005.

[17] J.P. Xue, R.Z. Pei, Numerical investigation of forced convection heat transfer in porous media using a thermal non-equilibrium model, Int. J. Heat Fluid Flow 22 (2001) 101–110.

[18] P. Zehner, E.U. Schlünder, Wärmeleifähigkeit von Schüttungen bei mässigen Temperaturen, Chem.-Ing.-Tech. 14 (1970) 933–941.